Identification of Benzo[a]pyrene(BaP)-Metabolizing Bacteria in Forest Soils Using DNA-Based Stable-Isotope Probing

Mengke Song [1], Chunling Luo [1*], Longfei Jiang [1], Dayi Zhang [2], Yujie Wang [3], Gan Zhang [1]

[1] Guangzhou Institute of Geochemistry, Chinese Academy of Sciences, Guangzhou 510640, China

[2] Lancaster Environment Centre, Lancaster University, Lancaster LA1 4YQ, UK

[3] School of Environmental Science and Engineering, Guangdong University of Technology, Guangzhou 510006, China

* Corresponding author: Dr. Chunling Luo

E-mail: clluo@gig.ac.cn; Tel.: +86-20-85290290; Fax: +86-20-85290706

Running Title: BaP Degraders Examined with SIP

ABSTRACT

DNA-based stable-isotope probing (DNA-SIP) was used in this study to investigate the uncultivated bacteria with benzo[a]pyrene (BaP) metabolism capacities in two Chinese forest soils (Mt. Maoer in Heilongjiang Province and Mt. Baicaowa in Hubei Province). Three different phylotypes were characterized with responsibility for BaP degradation, none of which was previously reported as BaP-degrading microorganisms by SIP. In Mt. Maoer soil microcosms, the putative BaP degraders were classified as belonging to the genus *Terrimonas* (family *Chitinophagaceae*, order *Sphingobacteriales*), whereas *Burkholderia* were the key BaP degraders in Mt. Baicaowa soils. The addition of metabolic salicylate significantly increased BaP degradation efficiency in Mt. Maoer soils, and the BaP-metabolizing bacteria shifted to the microorganisms in the family *Oxalobacteraceae* (genus unclassified). Meanwhile, salicylate addition did not change either BaP degradation or putative BaP degraders in Mt. Baicaowa. Polycyclic aromatic hydrocarbon-ring hydroxylating dioxygenase (PAH-RHD) genes were amplified, sequenced and quantified in the DNA-SIP ^{13}C heavy fraction to further confirm the BaP metabolism. By discussing the microbial diversity and salicylate additive effects on BaP degradation across different soils, the results increased our understanding of BaP natural attenuation and provided possible approach to enhance the bioremediation of BaP-contaminated soils.

Keywords: stable isotope probing (SIP), benzo[a]pyrene (BaP), forest soil, PAH-RHD gene, salicylate

INTRODUCTION

Polycyclic aromatic hydrocarbons (PAHs), a class of persistent organic pollutants (POPs), enter the environment through both natural and anthropogenic pathways. PAHs are released into the environment by means of natural processes such as forest fires and direct biosynthesis under the action of microbes and plants (1). The primary artificial source of PAHs is the incomplete combustion of organic matter at high temperatures caused by human activities (2). Their presence in the environment poses a severe threat to public and ecosystem health because of their known acute toxicity, and mutagenic, teratogenic, and carcinogenic features; they are therefore classified as priority pollutants by the U.S. Environmental Protection Agency (3). Furthermore, the persistence and genotoxicity of PAHs increase with molecular weight, and the presence of high-molecular-weight (HMW) PAHs in the environment is of greater concern. Benzo[a]pyrene (BaP), a representative HMW PAH with a five-ring structure, is a widespread pollutant with potent mutagenic and carcinogenic properties (4, 5). BaP is therefore identified as the first class of ‘‘human carcinogens’’ according to the report of the World Health Organization (WHO) International Agency for Research on Cancer (6). Generally, in soils with no industrial contamination, BaP concentrations vary from 3.5 to 3700 μg/kg, with a median concentration of 16 μg/kg soil; in contaminated soils and sediments, BaP concentrations range from 82 to 536 mg/kg (7).

Bacteria possessing the ability of BaP utilization are readily isolated from

contaminated soils or sediments, and most of our current knowledge about BaP metabolism by microbes has been gained from such isolates (8-10). The functional PAH-RHD genes (encoding PAH-ring hydroxylating dioxygenase enzymes) have also been examined to understand BaP degradation mechanisms, such as *nah*, *pah*, *arh* and *phn* genes in Gram-negative (GN) bacteria and the evolutionarily correlated *nid*, *nir*, *phd* and *nar* genes in Gram-positive (GP) bacteria, which are responsible for the first step of PAHs (naphthalene, phenanthrene, anthracene and pyrene) hydroxylation under aerobic conditions (11, 12). Terminal dioxygenase is the component of PAH-RHD, composed of large α and small β subunits. The genes coding for the mononuclear iron-containing catalytic domain (a conserved regions) of PAH-RHDα (α-subunit) have been widely used for studying RHD diversity and the PAH-degradation potential by bacteria in environment (11). In addition to the research on the genes involved in PAH degradation, studies using culture-dependent tools to investigate the degrading capacity of BaP degraders showed that rare bacteria were capable of metabolizing BaP without metabolic intermediate additives (9, 10, 13); in most cases, BaP degradation is stimulated by the addition of some intermediates produced during BaP metabolism (14, 15). These intermediates possess the ability of stimulating PAH dioxygenase activity and are capable of supplying electrons for nicotinamide adenine dinucleotide (NADH) coenzymes, which are necessary for the functions of oxygenase enzymes, to initiate aerobic PAH degradation (8, 16). Salicylate is a classic intermediate, inducing PAHs metabolism of PAHs-degrading bacteria and selectively stimulating their growth (8, 16, 17). The addition of salicylate

to contaminated soils or sediments has been proposed as a means of encouraging PAH degradation during bioremediation (16). *Sphingomonas yanoikuyae* JAR02 was reported to completely remove BaP (1.2 mg/L) within 20 h in the aqueous phase with additive salicylate (8). Additionally, *Pseudomonas saccharophila* P15 isolated from creosote-contaminated soil improved BaP removal after the addition of salicylate, which acted as the inducer of PAH dioxygenase activity (16).

The traditional culture-dependent approaches, such as isolating and cultivating target bacteria in the laboratory, suffer from the fact that <1% of the soil microorganisms are cultivable. The process underestimates the diversity of the prokaryotes and fails to capture the true nature of the complex interactions within microbial communities at a specific site. The uncultured bacteria may possess an unexplored reservoir of novel and valuable gene-encoding catalysts that benefit bioremediation, industry, and medicine (18-20). Furthermore, with our limited understanding of the actual biota, cultivation presents challenges for field bioremediation (21). In recent years, stable-isotope probing (SIP) has emerged as a culture-independent method to identify microorganisms capable of utilizing specific substrates in complex environments. Microbial populations responsible for the degradation of targeted contaminants are labeled by stable isotopes and then characterized (22-25). To date, many bacteria have been successfully identified by SIP with their unique capabilities of metabolizing phenolic compounds and PAHs, such as naphthalene (25, 26), anthracene (27), phenanthrene (26), pyrene (23, 28), fluoranthene (29), benz[a]anthracene (29), biphenyl (30, 31), phenol (31), and

benzoate (31). However, to our knowledge, no study till now has examined BaP-degrading bacteria successfully using SIP.

In the present study, to investigate the microorganisms responsible for BaP degradation in the uncontaminated soil, ^{13}C-DNA-targeted SIP was applied to two Chinese forest soils from Mt. Maoer and Mt. Baicaowa. The influence of salicylate on BaP biodegradation was further studied, as well as its role in functional microbial community dynamics. By sequencing and quantifying (by real-time polymerase chain reaction, qPCR) PAH-RHDα genes in ^{13}C-DNA enriched fraction, our work further revealed the BaP metabolism in uncontaminated soil and the stimulating effects of salicylate addition varying among different soils. To our knowledge, this study successfully apply the culture-independent SIP technique to characterize BaP-degrading bacteria in forest soil, and provides an important contribution to the understanding of BaP biodegradation in complex communities and the bioremediation of HMW PAHs-contaminated soil.

MATERIALS AND METHODS

Soil samples. Soil samples were collected from Mt. Maoer (45°22′48″N, 127°40′48″E) in Heilongjiang Province, and Mt. Baicaowa (40°48′36″N, 117°35′60″E) in Hebei Province, China. The pH and total organic carbon content were 7.5 and 16.0% (Mt. Maoer), and 6.0 and 12.3% (Mt. Baicaowa), respectively. Before use, large objects in the soils, such as stones and debris, were removed manually in the laboratory. The soil samples were then homogenized, sieved through a 2-mm

pore-size screen, and prepared for the BaP-degradation treatment.

Setup of BaP-degrading microcosms. Both non-salicylate and salicylate-additive treatments were included for the two forest soils. Hereafter, BS and B represent the Mt. Baicaowa soils amended with and without salicylate, and MS and M denote the Mt. Maoer soils amended with and without salicylate, respectively. The experiments were conducted as follows: Three grams of soil (dry weight) was placed in a 150-mL serum bottle containing 10 mL phosphate-buffered mineral medium (32). The bottles were sealed with rubber stoppers and compressed with an aluminum seal. The unlabeled BaP (99%) or ^{13}C-labeled BaP ($^{13}C_4$-BaP, 99%, Fig. S1 shows the position of ^{13}C-labeled carbons), both from Cambridge Isotope Laboratories, Inc. and dissolved in nonane with a final concentration of 100 mg/l, was added to the respective bottles using a gastight syringe to give a final BaP concentration of 1 mg/kg. For salicylate-additive treatments, the final salicylate concentration was 10 mg/kg. Two negative control treatments were included as no-carbon-source (CK) and non-bioactive (sterilized by γ -irradiation, ^{12}C-NB). Two positive treatments were amended with ^{12}C- and ^{13}C-labeled BaP carbon sources, named as ^{12}C-BT and ^{13}C-BT, respectively. Eight samples were prepared for each treatment. The microcosms were incubated at room temperature (~25 ℃) with reciprocal shaking at a speed of 120 rpm/min. On Day 7, 14, 28, and 42 after incubation, two samples from each treatment were sacrificed for BaP analysis and DNA extraction, respectively. All stock solutions were filtered through 0.2-μm pore-size filters and stored in dark-brown containers. To prepare sterile controls, soils were γ-irradiated (50 kGy) for 2 h before use.

BaP analysis. The ^{12}C-NB, ^{12}C-BT and ^{13}C-BT samples were prepared for BaP analysis using the following steps: The serum bottles were frozen at -20 ℃ overnight, followed by freeze-drying using a vacuum freeze dryer. The dry soil samples were then homogenized, pulverized, spiked with 1,000 ng of deuterated PAHs as surrogate standards and extracted with dichloromethane (DCM) in a Soxhlet apparatus for 48 h, with the addition of activated copper to remove sulfur. The extract was concentrated to ~0.5 mL after solvent exchange to hexane. The soil extracts were purified in a multilayer silica gel/alumina column (8 mm i.d.) filled with anhydrous Na_2SO_4 (1 cm), neutral silica gel (3 cm, 3% w/w; deactivated), and neutral alumina (3 cm, 3% w/w; deactivated; from top to bottom) via elution with 15 mL hexane/DCM (1:1, v/v). After concentrating to ~50 μL under a gentle stream of N_2, 1,000 ng of hexamethylbenzene was added as an internal standard prior to analysis.

BaP was detected on an Agilent 7890 gas chromatograph equipped with a capillary column (DB-5MS, 30 m, 0.25 mm, 0.25 μm) and a mass spectrometric detector (MSD, Agilent 5975). One microliter of sample was injected in splitless mode with a 10-min solvent delay time. High-purity helium was used as the carrier gas at a flow rate of 1.83 mL/min. The temperature of the injector and transfer lines was 290 and 300 ℃, respectively. The initial oven temperature was set at 60 ℃ for 1 min, rising to 290 ℃ at a rate of 3 ℃/min, and was subsequently held constant for 20 min. PAH standards were used to quantify BaP. Instrumental performance was subjected to quality-control calibration with the standards after each set of eight samples had been analyzed. Six PAHs standard concentrations were used to derive the

calibration curves. Concentrations were corrected using reference to surrogate recovery levels.

DNA extraction and ultracentrifugation. Samples from ^{12}C-BT and ^{13}C-BT were both prepared for biotic analysis at 7, 14, 28, and 42 days of cultivation. The total genomic DNA was extracted from 1.0 g soils with triplicates using the Powersoil® DNA Isolation Kit (MO BIO Laboratories, Inc.) according to the manufacturer's protocol. DNA concentrations were determined using an ND-2000 UV-Vis spectrophotometer (NanoDrop Technologies). Subsequently, ~10,000 ng DNA was added to Quick-Seal polyallomer tubes (13 × 51 mm, 5.1 mL, Beckman Coulter), along with a Tris-EDTA (TE, pH 8.0)/cesium chloride (CsCl) solution. Before the tubes were sealed with cordless Quick-Seal® Tube Topper (Beckman Coulter), the average buoyant density (BD) of all prepared gradients was determined with an AR200 digital refractometer (Leica Microsystems Inc.) and adjusted to ~1.77 g/mL by adding a CsCl solution or Tris–EDTA buffer, if necessary. The tubes were transferred to an ultracentrifuge (Optima L-100XP, Beckman Coulter) and centrifuged at 178,000 × g (20 ℃) for 48 h. Following centrifugation, 150-μL fractions were collected from each tube using a fraction recovery system (Beckman Coulter). The BD of each fraction was measured, and the CsCl was further removed by glycogen-assisted ethanol precipitation (33).

PCR and terminal restriction fragment length polymorphism (TRFLP). The fractions were subjected to terminal restriction fragment length polymorphism (TRFLP) analysis using standard procedures (24). Briefly, DNA was amplified with

27F-FAM (5′-AGAGTTTGATCMTGGCTCAG; 5′ end-labeled with carboxyfluorescein) and 1492R (5′-GGTTACCTTGTTACGACTT) using the following PCR program: initial melting at 94 ℃ for 5 min, 30 amplification cycles at 94 ℃ for 30 s, 55 ℃ for 30 s, and 72 ℃ for 1.5 min, with a final extension at 72 ℃ for 10 min. After amplification, the presence of PCR products was confirmed by 1% agarose gel electrophoresis. The PCR products were purified using an EZNA Cycle-Pure Kit (Omega Bio-Tek, Inc.) following the manufacturer's instructions and digested with *Hae*III (New England Biolabs) for 4–5 h at 37 ℃. One nanogram of each labeled PCR product was analyzed on an ABI 3730 Genetic Analyzer (Applied Biosystems) running Peak Scanner software version 1.0 (Applied Biosystems). A GeneScan™ ROX 500™ set of internal standards (Applied Biosystems) was used. The percent abundance of each fragment was determined as previously described (30).

Identification of the PAH-RHD$_\alpha$ gene in microcosms and enumeration in SIP fractions. As the PAH-RHD$_\alpha$ genes possessed by GN and GP bacteria do not belong to a monophyletic cluster (12), the presence of the PAH-RHD$_\alpha$ genes was investigated using PAH-RHDα GP primers (641F 5'-CGGCGCCGACAAYTTYGTNGG, 933R 5'-GGGGAACACGGTGCCRTGDATRAA) and PAH-RHDα GN primers (610F 5'-GAGATGCATACCACGTKGGTTGGA, 911R 5'-AGCTGTTGTTCGGGAAGAYWGTGCMGTT) (32) on the heavy DNA fractions from B, BS, M and MS microcosms, respectively. A gradient PCR was performed

214 with annealing temperatures ranging from 52 to 62 ℃. Amplification reactions were
215 carried out in a volume of 50 μL, as previously described (12).

216 The copy number of the PAH-RHDα sequences in fractions from ^{13}C-labeled and
217 unlabeled DNA was determined by qPCR using the PAH-RHDα GP primers, because
218 only one strong and specific amplicon amplified with PAH-RHDα GP primers was
219 produced from the heavy fractions in M and MS microcosms in this work. The PCR
220 mix contained 10 μL SYBR Green® PCR Premix Ex Taq^{TM} II (TaKaRa Bio) and 1 μL
221 DNA template in a final volume of 20 μL. A standard curve was obtained by
222 producing 10 dilution series of plasmid pGEM-T Easy Vector sequences (10^2–10^8
223 copies; Promega) containing the PAH-RHDα gene detected in M and MS treatments
224 with the PAH-RHDα GP primers (641F 5'-CGGCGCCGACAAYTTYGTNGG, 933R
225 5'-GGGGAACACGGTGCCRTGDATRAA). The amplification reactions were
226 conducted using a two-step method in a 48-well optical plate on an Eco^{TM} real-time
227 PCR system (Illumina) as follows: denaturation for 10 min at 95 ℃, followed by 40
228 cycles of 10 s at 95 ℃, and 30 s at 60 ℃; then the SYBR Green signal intensities were
229 measured after the 30 s step at 60 ℃. At the end of the real-time PCR, a melting curve
230 analysis was performed by increasing the temperature from 55 to 95 ℃. For each
231 DNA sample, the average of three replicates was determined as the copy number per
232 fraction.

233 **Sequencing of partial PAH-RHDα and 16S rRNA genes.** The 16S rRNA genes
234 from the heavy fractions (^{13}C-labeled DNA, marked with ☆ in Fig. 1)
235 corresponding to the peak in Fig. 1A- Fig. 1D with the BD value of 1.7198 g/ml,

1.7203 g/ml, 1.7165 g/ml and 1.7100 g/ml, as well as the amplicons generated with the PAH-RHDα GP primer pair in M and MS treatments, were cloned and sequenced. Briefly, the 16S rRNA gene was amplified using a similar process to that described above, except the 27F-FAM primer was replaced by 27F. The purified PCR products were cloned into a pGEM-T Easy Vector and transformed into *Escherichia coli* JM 109 (TaKaRa Bio). *E. coli* clones were then grown on Luria-Bertani medium solidified with 15 g/L agar in the presence of 50 μg/L ampicillin for 16 h at 37°C, and finally 100 clones with inserts were selected to be sequenced. The plasmids with target genes were extracted using an EZNA Plasmid Mini-Kit (Omega Bio-Tek, Inc.), and the recombinants were selected using 0.8% agarose gel electrophoresis and sequenced on an ABI 3730 genetic analyzer using M13 primers. Sequence similarity searches and alignments were performed using the Basic Local Alignment Search Tool (BLAST) algorithm (National Center for Biotechnology Information) and Molecular Evolutionary Genetics Analysis (MEGA 5.1).

The obtained 16S rRNA gene and the partial RHD gene sequences are available in GenBank (accession numbers KM267480–KM267482 for partial 16S rRNA gene sequences of a 196-bp terminal restriction fragment (TRF) in B and BS treatments, 450-bp TRF in M treatment, and 216-bp TRF in MS treatment; KM267486 was used for the partial PAH-RHDα gene sequence).

RESULTS

BaP biodegradation in soils. BaP biodegradation in the four treatments (B, BS,

M and MS) is briefly listed in Table 1. The recovery rates of BaP during the extraction procedure were 80%-90% in this work (Table S2). The BaP concentration in sterile treatments showed less decline comparing to unsterilized treatments. For instance, the residual BaP were 80.6%, 72.6%, 81.0% and 69.7% for the ^{12}C-NB of B, BS, M and MS microcosms, respectively. Significant BaP biodegradation was observed in the unsterilized microcosms. For B and BS treatments (Table 1), BaP degradation achieved 16.6% and 18.1% respectively after 7 days cultivation, and 33.4% and 31.1% of BaP was removed after 28 days. No significant BaP degradation difference was found between the B and BS treatments throughout the whole process, indicating the limited impacts of salicylate on the capacities of BaP-degrading bacteria. The BaP degradation in M and MS treatments was much faster than those from Mt. Baicaowa. For example, 32.1% and 47.4% of BaP was removed in M and MS samples after 14 days cultivation, compared to the corresponding degradation efficiency of 24.9% and 23.0% in B and BS samples. Salicylate significantly accelerated BaP biodegradation in soils from Mt. Maoer, where BaP removal efficiency was 32.1%, 43.7%, and 45.7% in M treatments at 14, 28, and 42 days, compared to the corresponding 47.4%, 52.5%, and 55.8% in MS treatments (Table 1).

Microbial structure analysis via SIP and TRFLP. DNA extracts from ^{12}C-BT and ^{13}C-BT soil samples were subjected to ultracentrifugation and fractionation, followed by TRFLP for each fraction. The organisms responsible for ^{13}C assimilation were detected by the relative abundances of specific TRFs between the control (^{12}C-BT) and the treatment with ^{13}C-labeled BaP (^{13}C-BT) at all three sampling points

for each fraction.

In B microcosms, the TRFLP results (Fig. 1) indicated that the 196-bp *Hae*III TRF at higher buoyant densities (1.7176–1.7328 g/mL) was enriched at 7, 14, and 28 days (16.6%, 24.9%, and 33.4% BaP removal, respectively) in ^{13}C-BT samples and that its relative abundance increased with time. Such enrichment and increasing trend were not observed in the ^{12}C-BT controls. Additionally, the enrichment of the 196-bp *Hae*III TRF in the heavy fractions was also supported by their higher fluorescence intensity in the 28-day treatments (Fig. S2A), suggesting that ^{13}C was incorporated by the microorganisms represented by the 196-bp *Hae*III TRF. To identify the BaP-degrading bacteria and obtain the phylogenetic affiliation of the 196-bp *Hae*III TRF, the 16S rRNA clone library derived from the ^{13}C heavy fractions was sequenced, and the clones with the 193-bp *Hae*III TRF cut site matched the TRFLP results for the 196-bp TRFs. The slight difference (2–3 bases) between the measured fragment lengths and those predicted using sequence data has been noted in previous studies (24, 34, 35). Based on the comparative analyses of 16S rRNA, the bacteria represented by the 196-bp TRF were classified as members of the genus *Burkholderia* (Fig. S3). Additionally, a partial sequence with the predicted 213-bp *Hae*III cut site in the clone library was related to the class *Acidobacteria*. An additional member with the predicted 206-bp *Hae*III cut site in the clone library was related to the genus *Rhodanobacter* (Table S1).

In BS microcosms with salicylate addition, the bacteria represented by the 196-bp *Hae*III TRF were involved in BaP biodegradation, as shown by DNA-SIP. Fig. 1A

illustrates a clear increasing relative abundance of 196-bp *Hae*III TRF at higher BD (>1.7203 g/mL) in the ^{13}C-BT samples compared to the ^{12}C-BT at 7, 14, and 28 days. Furthermore, in the ^{13}C-BT samples after 28 days cultivation, the BD value of the strongest fluorescence intensity of the 196-bp *Hae*III TRF was higher than that of the ^{12}C-BT samples (Fig. S2B). When the 16S rRNA clone library derived from the ^{13}C heavy fractions was inspected (Table S1), 43 of the 100 clones with the predicted 193-bp *Hae*III cut site fell in the genus *Burkholderiales*. These clones were associated with BaP degradation, the same as the BaP degraders in B treatment. Additionally, three different clones with the predicted 362-, 217-, and 202-bp *Hae*III cut sites were classified within the order *Burkholderiales*, and one clone with the predicted 212-bp *Hae*III cut site shared 100% similarity with strain *Acidobacteria* Gp3, which also occurred in the heavy fraction of B treatment.

In M microcosms, the TRFLP fraction profiles (Fig. 1C) and the fluorescence intensity at 42 days (Fig. S2C) indicated relatively more abundant 450-bp *Hae*III TRF in the heavy fractions (BD >1.7121 g/mL) of ^{13}C-BT samples, but not in ^{12}C-BT samples. Furthermore, the relative abundance of the 450-bp *Hae*III TRF in the heavy fraction increased with time in ^{13}C-BT samples, and the magnitude of the increase was largest for the sample that had been left the longest. For the ^{12}C-BT samples, the increase occurred in the light fraction (BD <1.7045 g/mL), indicating ^{13}C-BaP assimilation by the bacteria represented by the 450-bp *Hae*III TRF. However, this was not the dominant TRFLP fragment in the heavy fractions from ^{13}C-BT samples, and the other three TRFs (237, 372, and 215 bp) were the major members. Nevertheless,

those microorganisms were not responsible for ^{13}C-BaP degradation since a similar abundance was found in the heavy fractions of the ^{12}C-BT samples. The sequence of 16S rRNA clone libraries with the predicted 447-bp cut site fit well with the TRFLP results. They were assigned to the genus *Terrimonas* (phylum *Bacteroidetes*, class *Sphingobacteria*, order *Sphingobacteriales*, family *Chitinophagaceae*), belonging most closely to the *Flavisolibacter ginsengiterrae* strain Gsoil 492 (Fig. S4). Three clones with predicted 237-, 372-, and 215-bp *Hae*III cut sites also appeared in the 16S rRNA clone library derived from the ^{13}C heavy fractions (Table S1), and they were classified in the genus *Spartobacteria incertae sedis*, class *Acidobacteriaceae* and family *Oxalobacteraceae*, respectively.

In MS treatment with salicylate addition, the 216-bp *Hae*III TRF was involved in the BaP biodegradation, and was enriched as the dominant TRF in the heavy fractions (BD >1.7056 g/mL) at 28 and 42 days (Fig. 1D and Fig. S2D). An increasing relative abundance was also observed for 14–42 days of cultivation in treatments amended with ^{13}C-BaP, but not in ^{12}C-BT samples (Fig. 1D). Such increase suggested that microorganisms represented by the 216-bp TRF were responsible for ^{13}C substrate uptake (^{13}C-BaP degradation). Additionally, the relative abundance and fluorescence intensity of the 77-, 200-, and 450-bp TRFs (Fig. S2D) were also high in the heavy fractions, but lower than the 216-bp TRF in the ^{13}C-BT samples. The BD values of the three TRFs and their trends of relative abundance were similar between ^{13}C-BT and ^{12}C-BT treatments at the three sampling times. Hence, the microorganisms represented by the three TRFs were not directly involved in BaP degradation, and the

large proportion of TRFs in the fractions might be due to their tolerance to BaP. Clones with the 216-bp *Hae*III cut site from 16S rRNA clone libraries matched the TRFLP results, classified as members of the family *Oxalobacteraceae* (phylum *Proteobacteria*, class *Betaproteobacteria*, order *Burkholderiales*) , also present in MS ^{13}C-BaP treatment, and sharing 98% sequence similarity with *Janthinobacterium lividum* strain DSM 1522 (Fig. S5). Clones with 77-, 200-, and 447-bp *Hae*III cut sites were classified in the order *Actinomycetales*, family *Burkholderiaceae*, and genus *Terrimonas*, respectively (Table S1-MS).

Occurrence and quantification of PAH-RHDα genes in the SIP fractions. In B, BS, M, and MS treatments, PAH-RHDα GP amplicons were only detected in the heavy fractions from the ^{13}C-BaP-amended M and MS microcosms with the primer pair of 641f and 933r (Fig. 2), although both PAH-RHDα GP and PAH-RHDα GN primers were used to amplify PAH-RHDα genes in all treatments. In both treatments, the PAH-RHDα gene (PAH-RHDα-M) sequences shared 99% similarity with those of an uncultured strain (KF656719.1), and also high sequence similarity with the affiliation to the genus *Mycobacterium* which was capable of degrading BaP (15, 36). Recently, the microbial metabolism of low-molecular-weight (LMW) PAHs with no more than three rings has been studied extensively, including their metabolic pathways, and enzymatic and genetic regulation (7). However, little is known about the metabolic pathways and genes related to BaP degradation and other HMW-PAHs (37). Therefore, not all the functional genes derived from the active BaP-degrading bacteria could be detected by the primer sets used in this study.

PAH-RHDα-M genes in M and MS treatments were quantified against each density-resolved fraction (Fig. 3). A marked enrichment of PAH-RHDα-M genes in the heavy fractions (BD >1.7200 g/mL) was observed in the ^{13}C-BaP-amended soils in MS treatment, indicating that the BD value of PAH-RHDα-M increased with ^{13}C-BaP degradation efficiency. In ^{12}C-BaP control, the majority of the PAH-RHDα-M genes were found in fractions with BD <1.7200 g/mL (Fig. 3A). For M treatment, no significant difference was observed between the ^{13}C-BT and ^{12}C-BT samples due to the limited changes in the PAH-RHDα-M genes and BD value (Fig. 3B). Hence, the detected PAH-RHDα-M genes were associated with BaP degradation in MS but not in M treatment, attributing to the salicylate addition, which significantly promoted the expression of PAH-RHDα-M genes, stimulated PAH-RHDα-M encoding bacteria and improved BaP biodegradation.

DISCUSSION

Microorganisms responsible for the BaP degradation. DNA-SIP has been widely applied to the identification of pollutant degraders in numerous environmental media and with an ever-expanding pool of compounds (22, 27, 38). In the present study, the coupling of DNA-SIP and TRFLP techniques revealed the bacteria correlated with BaP metabolism in soils from Mt. Maoer and Mt. Baicaowa. Bacteria represented by 196-bp TRF were classified as members of the genus *Burkholderia*, and involved in BaP degradation in both B and BS treatments. *Burkholderia*-related bacteria have been linked with PAHs (39) and biphenyl (40) biodegradation in soil.

As the dominant genus with key roles in the degradation of oil components (41), *Burkholderia* was found to be capable of degrading anthracene, phenanthrene, chrysene, and pyrene (7). Juhasz et al. found that a *Burkholderia cepacia* strain isolated from soil near a manufacturing gas plant could degrade BaP with pyrene as the carbon source, although only 1.4–6.2% BaP was removed after 56 days (42). A *Delftia* strain was isolated from the microbial consortium of a crude oil-contaminated soil and removed 56.6% BaP in PAH-contaminated soil after 14 days (43). To our knowledge, prior to this study, BaP degradation by *Burkholderia*-related microorganisms using DNA-SIP has not been documented.

In M treatment, microorganisms represented by the 450-bp TRF were correlated with BaP degradation and assigned to the genus *Terrimonas*. Sequence analysis suggested their close relationship to the *F. ginsengiterrae* strain Gsoil 492 (Fig. S4). This strain was first isolated by Yoon and Im from soil used for ginseng planting, and it has the ability for growth with 3-hydroxybenzoic or 4-hydroxybenzoic acid as the sole carbon source (44). Strains of the genus *Sphingomonas* from the family *Sphingomonadaceae*, order *Sphingomonadales*, were able to degrade BaP with different co-metabolic substances, and aqueous 1.2 mg/L BaP was completely removed within 20 h when *S. yanoikuyae* JAR02 grew on salicylate (8). Ye et al. also showed that 5% BaP was removed by *Sphingomonas paucimobilis* with fluoranthene as the co-metabolic source of carbon and energy after 168 h when the initial concentration of BaP was 10 mg/L (45). Until now, some strains affiliated to *Chitinophagaceae* were found in various environments and possessed the functions of

412 metabolizing complex organic compounds. Though the crucial roles of these strains in
413 carbon circulation were reported (46), little was known about their PAH-degrading
414 capabilities. The present study show that the genus *Terrimonas* correlated with BaP
415 degradation, which expand our knowledge of this genus.

416 The bacteria involved in BaP degradation in MS microcosm amended with BaP
417 and salicylate were affiliated most closely with the family *Oxalobacteraceae* (phylum
418 *Proteobacteria*, class *Betaproteobacteria*, order *Burkholderiales*, 216 bp). To date,
419 many *Pseudomonas* strains in γ-*Proteobacteria* have been shown to possess the
420 capability of degrading aromatic hydrocarbons such as pyrene, phenanthrene,
421 naphthalene, toluene, and phenol in crude oil-contaminated soil (47).
422 *Burkholderiales*-related bacteria in β-*Proteobacteria* were also related to PAHs
423 removal, and the family *Oxalobacteraceae* was widely found in PCBs- and
424 PAHs-contaminated soils (40, 48). Huang reported that a cultivated bacterial strain
425 from the class *Burkholderiales* could degrade PAHs (41). However, no previous
426 studies using SIP have demonstrated the BaP-degradation capacity of
427 *Burkholderiales*-related bacteria, and our results in Mt. Baicaowa soils suggest such
428 possibilities.

429 The coupling of TRFLP with SIP enabled us to compare the TRFLP profiles over
430 a range of BDs for both ^{13}C-labeled and unlabeled samples at different time intervals
431 to avoid false-positive results. For example, in the M treatment, although three clones
432 with predicted 237-, 372-, and 215-bp *Hae*III cut sites were dominant in the 16S
433 rRNA clone library, and the corresponding TRFs constituted a high proportion in the

^{13}C heavy fractions from ^{13}C-BaP-amended treatment, no significant difference was observed in these TRFs between the ^{13}C-BaP and ^{12}C-BaP treatments, suggesting their limited roles in *in situ* BaP degradation in our study.

The conflict between Gram-positive PAH-RHDα genes and detected Gram-negative BaP degraders is a puzzle. Such evolutionary distant has been explained previously as horizontal gene transfers of PAH-RHDα genes and other genes between Gram-positive and Gram-negative bacteria (49-52). For instance, the classical *nah*-like genes were shared among gram-negative bacteria (49). *aphA-3*, an antibiotic resistance gene in *Campylobacter* encoding 3'-aminoglycoside phosphotransferases modifying the structure of kanamycin, was transferred between gram-positive and gram-negative bacteria (53). In our study, SIP results could not directly affiliate the Gram-positive PAH-RHDα genes to the functional Gram-negative host, therefore not able to prove the evidence of horizontal gene transfer. Further work is suggested on the single-cell isolation and genome amplification of individual BaP degraders (54) and deeper investigation on the PAH-RHDα genes within the targeting functional species.

Effects of salicylate on BaP degradation and community structure. The addition of salicylate significantly changed the functional microbial community structure in the heavy fractions derived from the Mt. Baicaowa soils, but not the BaP degradation. The dominant species shifted from *Rhodanobacter*-related bacteria in B microcosm to *Burkholderiales*-related bacteria in BS treatment, although *Acidobacteria*-related microorganisms existed in both treatments. The bacteria

456 capable of degrading BaP (*Burkholderiales*) in B and BS treatments were detected as
457 identical using DNA-SIP (Table S1). Nevertheless, the similar BaP removal efficiency
458 between B and BS treatments hinted that BaP degradation was not stimulated by the
459 functional microbial structure change and increasing *Burkholderiales*-related bacteria,
460 consistent with a previous study by Powell (12). Since small pH variation might
461 significantly affect the biodegradation of xenobiotics and other organic compounds in
462 oligotrophic environments (55), the possible reason was the decreased PAHs
463 degradation activity of dominant *Burkholderiales*-related bacteria under low pH
464 conditions (56), like pH=6.0 in Mt. Baicaowa soils.

465 However, the TRFLP in M and MS treatments suggested that the addition of
466 salicylate changed both functional microbial community structure in heavy fractions
467 and BaP degradation rate (Table S1). The dominant species correlated with BaP
468 degradation shifted from *Terrimonas* to *Oxalobacteraceae* after the salicylate addition.
469 The functional PAH-RHD genes might change (Fig. 3), and salicylate also accelerated
470 the BaP degradation in Mt. Maoer microcosms (Table 1). Previous studies showed a
471 significant increase in the rate of naphthalene mineralization in soil after enrichment
472 with salicylate spiking (38). The presence of phenanthrene and salicylate also greatly
473 enhanced the initial removal rates of benz[a]anthracene, chrysene, and
474 benzo[a]pyrene by *P. saccharophila* P15 (16). The addition of salicylate to
475 PAHs-contaminated soils was shown to increase the quantity of
476 naphthalene-degrading bacteria (57, 58), and stimulate the degradation of
477 benzo[a]anthracene, chrysene (16), fluoranthene (16, 17), and BaP (8, 16).

Salicylate was also reported to sustain populations of biological control bacteria with naphthalene-degrading genes in agricultural systems (59), and various salicylate additives (spiked or slow/continuous addition) have been used to select different microbial communities (38).

The effects of salicylate on PAHs removal and functional microbial community structure depend on the soil properties and the bacterial profiles in the soils. Although salicylate is the central metabolite of many PAHs-degradation processes, it is not associated with some pathways, and its stimulating effect, therefore, might not be suitable for all cases of PAHs degradation. For example, the addition of salicylate had no effect on phenanthrene or pyrene removal in PAHs-contaminated soils (60). After enrichment with salicylate, the initial naphthalene mineralization rate rather than phenanthrene and BaP, was enhanced by the microbial community in a bioreactor for a PAHs-contaminated soil treatment (38). While, in uncontaminated soils, salicylate only improved pyrene removal but did not affect BaP (60), which may explain why salicylate stimulated BaP removal in Mt. Maoer soils, but not Mt. Baicaowa.

In summary, three phylotypes in two different forest soils were linked with BaP degradation using the culture-independent SIP technique. The addition of salicylate affected the bacteria correlated with BaP metabolism and the BaP degradation efficiency differently in the two forest soils. Besides, a new PAH-RHDα gene involved in BaP metabolism was detected in the salicylate-amended soils from Mt. Maoer. Our results provide a deeper understanding of the contribution of SIP to identifying the functions of uncultured microorganisms, expand our knowledge on

bacteria possessing the ability of BaP mineralization, and reveal specific effects of salicylate on the BaP-biodegradation process.

ACKNOWLEDGEMENT

This study was supported by the Joint Funds of the National Natural Science Foundation of China and the Natural Science Foundation of Guangdong Province, China (No. U1133004), the National Natural Science Foundation of China (Nos. 41173082 & 41322008), and the Scientific and Technological Planning Project of Guangzhou, China (No. 201510010038).

REFERENCE

1. **Baek SO, Field RA, Goldstone ME, Kirk PW, Lester JN, Perry R.** 1991. A Review of Atmospheric Polycyclic Aromatic-Hydrocarbons - Sources, Fate and Behavior. Water Air Soil Poll **60:**279-300.
2. **Zhang YX, Tao S.** 2009. Global atmospheric emission inventory of polycyclic aromatic hydrocarbons (PAHs) for 2004. Atmos Environ **43:**812-819.
3. **Keith LH, Telliard WA.** 1979. Priority Pollutants I-a Perspective View. Environ Sci Technol **13:**416-423.
4. **Rodriguez-Fragoso L, Melendez K, Hudson LG, Lauer FT, Burchiel SW.** 2009. EGF-receptor phosphorylation and downstream signaling are activated by benzo[a]pyrene 3,6-quinone and benzo[a]pyrene 1,6-quinone in human mammary epithelial cells. Toxicol Appl Pharm **235:**321-328.
5. **Wills LP, Zhu SQ, Willett KL, Di Giulio RT.** 2009. Effect of CYP1A inhibition on the biotransformation of benzo[a]pyrene in two populations of Fundulus heteroclitus with different exposure histories. Aquat Toxicol **92:**195-201.
6. **Anonymous.** 2010. Iarc Monographs on the Evaluation of Carcinogenic Risks to Humans. Iarc Monog Eval Carc **95:**9-38.
7. **Juhasz AL, Naidu R.** 2000. Bioremediation of high molecular weight polycyclic aromatic hydrocarbons: a review of the microbial degradation of benzo[a]pyrene. Int Biodeter Biodegr **45:**57-88.
8. **Rentz JA, Alvarez PJJ, Schnoor JL.** 2008. Benzo[a]pyrene degradation by Sphingomonas yanoikuyae JAR02. Environ Pollut **151:**669-677.
9. **Peng H, Yin H, Deng J, Ye JS, Chen SN, He BY, Zhang N.** 2012. Biodegradation of Benzo[a]pyrene by Arthrobacter oxydans B4. Pedosphere **22:**554-561.
10. **Mishra S, Singh SN.** 2014. Biodegradation of benzo(a)pyrene mediated by catabolic enzymes of bacteria. Int J Environ Sci Te **11:**1571-1580.
11. **Jurelevicius D, Alvarez VM, Peixoto R, Rosado AS, Seldin L.** 2012. Bacterial polycyclic aromatic hydrocarbon ring-hydroxylating dioxygenases (PAH-RHD) encoding genes in different soils from King George Bay, Antarctic Peninsula. Appl Soil Ecol **55:**1-9.
12. **Cebron A, Norini MP, Beguiristain T, Leyval C.** 2008. Real-Time PCR quantification of PAH-ring hydroxylating dioxygenase (PAH-RHD alpha) genes from Gram positive and Gram negative bacteria in soil and sediment samples. J Microbiol Meth **73:**148-159.
13. **Lily MK, Bahuguna A, Dangwal K, Garg V.** 2009. Degradation of Benzo [a] Pyrene by a Novel Strain Bacillus Subtilis Bmt4i (Mtcc 9447). Braz J Microbiol **40:**884-892.
14. **Kanaly RA, Harayama S.** 2000. Biodegradation of high-molecular-weight polycyclic aromatic hydrocarbons by bacteria. J Bacteriol **182:**2059-2067.
15. **Kanaly RA, Harayama S.** 2010. Advances in the field of high-molecular-weight polycyclic aromatic hydrocarbon biodegradation by bacteria. Microb Biotechnol **3:**136-164.
16. **Chen SH, Aitken MD.** 1999. Salicylate stimulates the degradation of high molecular weight polycyclic aromatic hydrocarbons by Pseudomonas saccharophila P15. Environ Sci Technol **33:**435-439.
17. **Alemayehu D, Gordon LM, O'Mahony MM, O'Leary ND, Dobson ADW.** 2004. Cloning and functional analysis gene involved in indigo production by gene disruption of a novel and fluoranthene metabolism in Pseudomonas alcaligenes PA-10. Fems Microbiol Lett **239:**285-293.

554 18. **Bode HB, Muller R.** 2005. The impact of bacterial genomics on natural product research. Angew
555 Chem Int Edit **44:**6828-6846.
556 19. **Galvao TC, Mohn WW, de Lorenzo V.** 2005. Exploring the microbial biodegradation and
557 biotransformation gene pool. Trends Biotechnol **23:**497-506.
558 20. **Lorenz P, Eck J.** 2005. Metagenomics and industrial applications. Nat Rev Microbiol **3:**510-516.
559 21. **Oren A.** 2004. Prokaryote diversity and taxonomy: current status and future challenges. Philos T
560 Roy Soc B **359:**623-638.
561 22. **Radajewski S, Ineson P, Parekh NR, Murrell JC.** 2000. Stable-isotope probing as a tool in
562 microbial ecology. Nature **403:**646-649.
563 23. **Singleton DR, Sangaiah R, Gold A, Ball LM, Aitken MD.** 2006. Identification and quantification of
564 uncultivated Proteobacteria associated with pyrene degradation in a bioreactor treating
565 PAH-contaminated soil. Environ Microbiol **8:**1736-1745.
566 24. **Luo CL, Xie SG, Sun WM, Li XD, Cupples AM.** 2009. Identification of a Novel Toluene-Degrading
567 Bacterium from the Candidate Phylum TM7, as Determined by DNA Stable Isotope Probing. Appl
568 Environ Microb **75:**4644-4647.
569 25. **Gutierrez T, Singleton DR, Aitken MD, Semple KT.** 2011. Stable Isotope Probing of an Algal
570 Bloom To Identify Uncultivated Members of the Rhodobacteraceae Associated with
571 Low-Molecular-Weight Polycyclic Aromatic Hydrocarbon Degradation. Appl Environ Microb
572 **77:**7856-7860.
573 26. **Singleton DR, Powell SN, Sangaiah R, Gold A, Ball LM, Aitken MD.** 2005. Stable-isotope probing
574 of bacteria capable of degrading salicylate, naphthalene, or phenanthrene in a Bioreactor
575 treating contaminated soil. Appl Environ Microb **71:**1202-1209.
576 27. **Zhang SY, Wang QF, Xie SG.** 2012. Stable isotope probing identifies anthracene degraders under
577 methanogenic conditions. Biodegradation **23:**221-230.
578 28. **Peng JJ, Zhang Y, Su JQ, Qiu QF, Jia ZJ, Zhu YG.** 2013. Bacterial communities predominant in the
579 degradation of C-13(4)-4,5,9,10-pyrene during composting. Bioresource Technol **143:**608-614.
580 29. **Jones MD, Crandell DW, Singleton DR, Aitken MD.** 2011. Stable-isotope probing of the polycyclic
581 aromatic hydrocarbon-degrading bacterial guild in a contaminated soil. Environ Microbiol
582 **13:**2623-2632.
583 30. **Sul WJ, Park J, Quensen JF, Rodrigues JLM, Seliger L, Tsoi TV, Zylstra GJ, Tiedje JM.** 2009.
584 DNA-Stable Isotope Probing Integrated with Metagenomics for Retrieval of Biphenyl Dioxygenase
585 Genes from Polychlorinated Biphenyl-Contaminated River Sediment. Appl Environ Microb
586 **75:**5501-5506.
587 31. **Uhlik O, Wald J, Strejcek M, Musilova L, Ridl J, Hroudova M, Vlcek C, Cardenas E, Mackova M,**
588 **Macek T.** 2012. Identification of Bacteria Utilizing Biphenyl, Benzoate, and Naphthalene in
589 Long-Term Contaminated Soil. Plos One **7**.
590 32. **Mu DY, Scow KM.** 1994. Effect of Trichloroethylene (Tce) and Toluene Concentrations on Tce and
591 Toluene Biodegradation and the Population-Density of Tce and Toluene Degraders in Soil. Appl
592 Environ Microb **60:**2661-2665.
593 33. **Sun WM, Xie SG, Luo CL, Cupples AM.** 2010. Direct Link between Toluene Degradation in
594 Contaminated-Site Microcosms and a Polaromonas Strain. Appl Environ Microb **76:**956-959.
595 34. **Cupples AM, Sims GK.** 2007. Identification of in situ 2,4-dichlorophenoxyacetic acid-degrading
596 soil microorganisms using DNA-stable isotope probing. Soil Biol Biochem **39:**232-238.
597 35. **Sun WM, Cupples AM.** 2012. Diversity of Five Anaerobic Toluene-Degrading Microbial

598 Communities Investigated Using Stable Isotope Probing. Appl Environ Microb **78:**972-980.
599 36. **Warshawsky D, Ladow K, Schneider J.** 2007. Enhanced degradation of benzo[a]pyrene by
600 Mycobacterium sp in conjunction with green alga. Chemosphere **69:**500-506.
601 37. **Moody JD, Freeman JP, Fu PP, Cerniglia CE.** 2004. Degradation of benzo[a]pyrene by
602 Mycobacterium vanbaalenii PYR-1. Appl Environ Microb **70:**340-345.
603 38. **Powell SN, Singleton DR, Aitken MD.** 2008. Effects of enrichment with salicylate on bacterial
604 selection and PAH mineralization in a microbial community from a bioreactor treating
605 contaminated soil. Environ Sci Technol **42:**4099-4105.
606 39. **Ang EL, Zhao HM, Obbard JP.** 2005. Recent advances in the bioremediation of persistent organic
607 pollutants via biomolecular engineering. Enzyme Microb Tech **37:**487-496.
608 40. **de Carcer DA, Martin M, Karlson U, Rivilla R.** 2007. Changes in bacterial populations and in
609 biphenyl dioxygenase gene diversity in a polychlorinated biphenyl-polluted soil after introduction
610 of willow trees for rhizoremediation. Appl Environ Microb **73:**6224-6232.
611 41. **Huang X, Luo Y, Hu Z, Tian Y.** 2006. Recent advance in the study of persistent organic pollutants
612 bioremediation. Acta Sci Circum **26:**353-361.
613 42. **Juhasz AL, Britz ML, Stanley GA.** 1997. Degradation of benzo[a]pyrene, dibenz[a,h]anthracene
614 and coronene by Burkholderia cepacia. Water Sci Technol **36:**45-51.
615 43. **Zafra G, Absalon AE, Cuevas MD, Cortes-Espinosa DV.** 2014. Isolation and Selection of a Highly
616 Tolerant Microbial Consortium with Potential for PAH Biodegradation from Heavy Crude
617 Oil-Contaminated Soils. Water Air Soil Poll **225**.
618 44. **Yoon MH, Im WT.** 2007. Flavisolibacter ginsengiterrae gen. nov., sp nov and Flavisolibacter
619 ginsengisoli sp nov., isolated from ginseng cultivating soil. Int J Syst Evol Micr **57:**1834-1839.
620 45. **Ye DY, Siddiqi MA, Maccubbin AE, Kumar S, Sikka HC.** 1996. Degradation of polynuclear
621 aromatic hydrocarbons by Sphingomonas paucimobilis. Environ Sci Technol **30:**136-142.
622 46. **Everard A, Lazarevic V, Derrien M, Girard M, Muccioli GG, Neyrinck AM, Possemiers S, Van**
623 **Holle A, Francois P, de Vos WM, Delzenne NM, Schrenzel J, Cani PD.** 2011. Responses of gut
624 microbiota and glucose and lipid metabolism to prebiotics in genetic obese and diet-induced
625 leptin-resistant mice. Diabetes **60:**3307-3307.
626 47. **Chang. H, Nie. M, Ge. B, Liu. C, Yang. Q, Zhou. L, Fan. X, Sun. C.** 2013. Effects of rhamnolipid on
627 oil degradation by Pseudomonas aeruginosa strain NY3. Chin J Environ Eng **7:**771-776.
628 48. **Tejeda-Agredano MC, Gallego S, Vila J, Grifoll M, Ortega-Calvo JJ, Cantos M.** 2013. Influence of
629 the sunflower rhizosphere on the biodegradation of PAHs in soil. Soil Biol Biochem **57:**830-840.
630 49. **Habe H, Omori T.** 2003. Genetics of polycyclic aromatic hydrocarbon metabolism in diverse
631 aerobic bacteria. Biosci Biotech Bioch **67:**225-243.
632 50. **Herrick JB, StuartKeil KG, Ghiorse WC, Madsen EL.** 1997. Natural horizontal transfer of a
633 naphthalene dioxygenase gene between bacteria native to a coal tar-contaminated field site.
634 Appl Environ Microb **63:**2330-2337.
635 51. **Wilson MS, Herrick JB, Jeon CO, Hinman DE, Madsen EL.** 2003. Horizontal transfer of phnAc
636 dioxygenase genes within one of two phenotypically and genotypically distinctive
637 naphthalene-degrading guilds from adjacent soil environments. Appl Environ Microb
638 **69:**2172-2181.
639 52. **Yagi JM, Sims D, Brettin T, Bruce D, Madsen EL.** 2009. The genome of Polaromonas
640 naphthalenivorans strain CJ2, isolated from coal tar-contaminated sediment, reveals
641 physiological and metabolic versatility and evolution through extensive horizontal gene transfer.

Environ Microbiol **11:**2253-2270.

53. **Trieucuot P, Gerbaud G, Lambert T, Courvalin P.** 1985. Invivo Transfer of Genetic Information between Gram-Positive and Gram-Negative Bacteria. Embo J **4:**3583-3587.
54. **Zhang DY, Berry JP, Zhu D, Wang Y, Chen Y, Jiang B, Huang S, Langford H, Li GH, Davison PA, Xu J, Aries E, Huang WE.** 2015. Magnetic nanoparticle-mediated isolation of functional bacteria in a complex microbial community. Isme J **9:**603-614.
55. **Kastner M, Breuer-Jammali M, Mahro B.** 1998. Impact of inoculation protocols, salinity, and pH on the degradation of polycyclic aromatic hydrocarbons (PAHs) and survival of PAH-degrading bacteria introduced into soil. Appl Environ Microb **64:**359-362.
56. **Wong JWC, Lai KM, Wan CK, Ma KK, Fang M.** 2002. Isolation and optimization of PAH-degradative bacteria from contaminated soil for PAHs bioremediation. Water Air Soil Poll **139:**1-13.
57. **Ogunseitan OA, Delgado IL, Tsai YL, Olson BH.** 1991. Effect of 2-Hydroxybenzoate on the Maintenance of Naphthalene-Degrading Pseudomonads in Seeded and Unseeded Soil. Appl Environ Microb **57:**2873-2879.
58. **Ogunseitan OA, Olson BH.** 1993. Effect of 2-Hydroxybenzoate on the Rate of Naphthalene Mineralization in Soil. Appl Microbiol Biot **38:**799-807.
59. **Ji PS, Wilson M.** 2003. Enhancement of population size of a biological control agent and efficacy in control of bacterial speck of tomato through salicylate and ammonium sulfate amendments. Appl Environ Microb **69:**1290-1294.
60. **Carmichael LM, Pfaender FK.** 1997. The effect of inorganic and organic supplements on the microbial degradation of phenanthrene and pyrene in soils. Biodegradation **8:**1-13.

FIGURE AND TABLE LEGENDS

Table

Table 1. Percentage of BaP remaining in soils over time

Figures

Fig. 1 Relative abundance of TRFLP fragments (digested by HaeIII) assigned to *Burkholderia1* (A), *Burkholderia2* (B), *Terrimonas* (C), *Oxalobacteraceae* (D) against the buoyant density gradients in B, BS, M and MS treatments.

Fig. 2 Phylogenetic tree of PAH-RHDα-M genes from MS (microcosms from Mt. Maoer soil amended with salicylate) and M (microcosms from Mt. Maoer soil without salicylate) treatments along with the closest matches in GenBank, constructed with MEGA 5.0 software using the neighbor-joining method.

Fig. 3 PAH-RHDα-M gene copies in ultracentrifugation fractions from ^{13}C-BaP and ^{12}C-BaP amended microcosms determined by qPCR. A and B represent the microcosms from Mt. Maoer soil with/without salicylate addition. Figure symbols: □ ^{13}C-BaP (~52% BaP degraded); ■ ^{12}C-BaP (~42% BaP degraded).

682 **Table 1.** Percentage of BaP remaining in soils over time

Time (days)	B(%)			BS(%)			M(%)			MS(%)		
	^{12}C-NB	^{12}C-BT	^{13}C-BT	^{12}C-NB	^{12}C-BT	^{13}C-BT	^{12}C-NB	^{12}C-BT	^{13}C-BT	^{12}C-NB	^{12}C-BT	^{13}C-BT
7	87.1	70.5	71.3	85.3	67.2	66.3	-	-	-	-	-	-
14	78.4	53.5	52.7	83.1	60.1	62.1	88.9	56.8	59.7	72.9	25.6	24.8
28	80.6	47.2	48.6	72.6	41.5	41.5	82.0	38.3	37.9	70.4	17.9	18.2
42	-	-	-	-	-	-	81.0	35.4	36.4	69.7	13.9	11.7

683 Note: ^{12}C-NB represents the non-bioactive autoclaved treatment; ^{12}C-BT represents the treatment with ^{12}C-BaP as the sole carbon sources; ^{13}C-BT represents the treatment
684 with ^{13}C-BaP as the sole carbon sources. B and BS represent the soil microcosms from Mt. Baicaowa amended without/with salicylate, whereas M and MS refer to the
685 soil microcosms from Mountain Maoer amended without/with salicylate. " - " means samples were not set at the time.

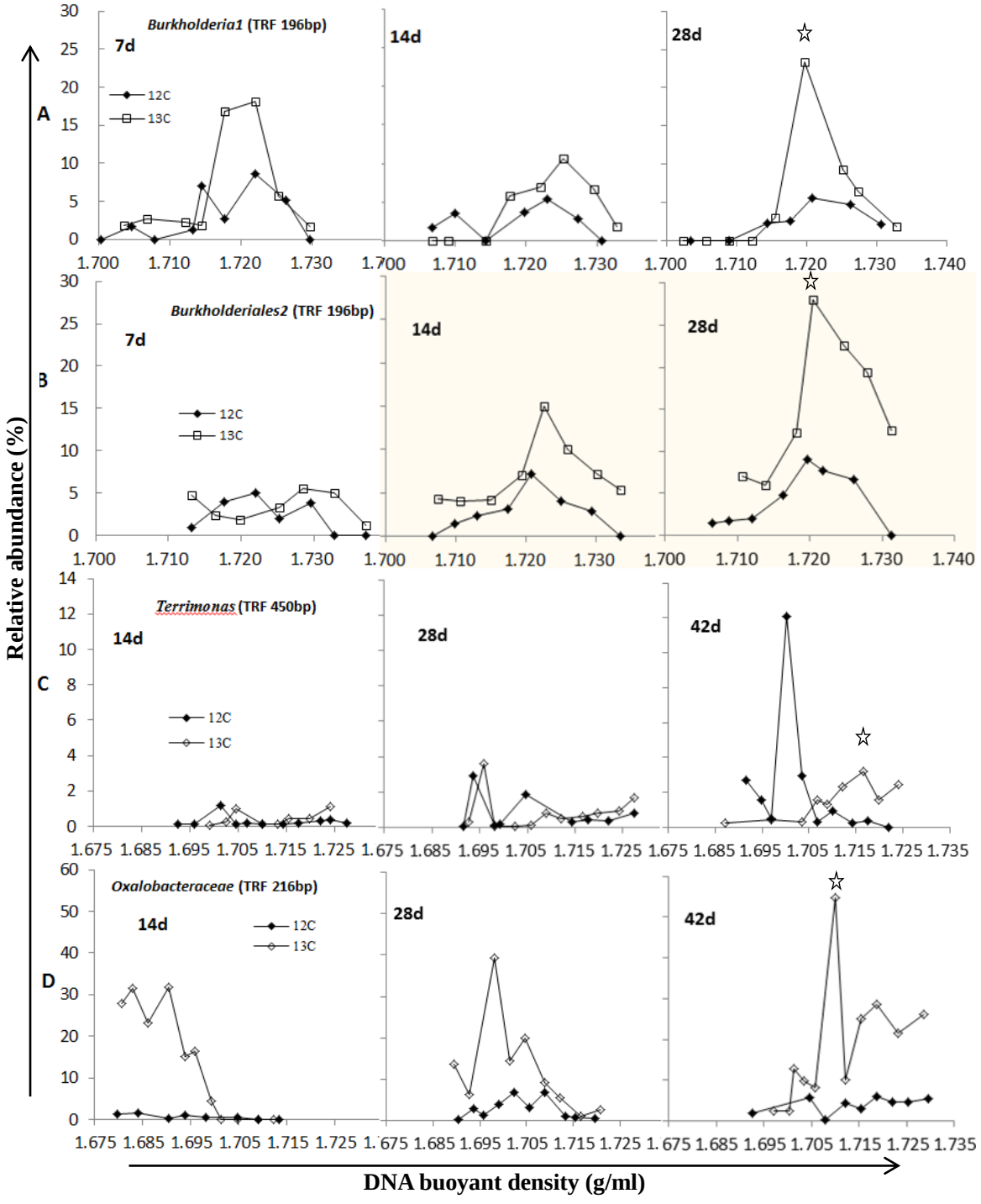

Fig. 1. Relative abundance of TRFLP fragments (digested by HaeIII) assigned to *Burkholderia1* (A), *Burkholderia2* (B), *Terrimonas* (C), *Oxalobacteraceae* (D) against the buoyant density gradients in B, BS, M and MS treatments. The bacterial DNA were extracted from B (microcosms from Mt. Baicaowa soil) and BS (microcosms from Mt. Baicaowa soil amended with salicylate) after 7, 14 and 28 days, and M (microcosms from Mt. Maoer soil) and MS (microcosms from Mt. Maoer soil amended with salicylate) after 14, 28 and 42 days. Figure symbols: □ ^{13}C-BaP; ■ ^{12}C-BaP. ☆ shows the fractions used for sequencing of partial PAH-RHDα and 16S rRNA genes involved in BaP degradation in all the treatments.

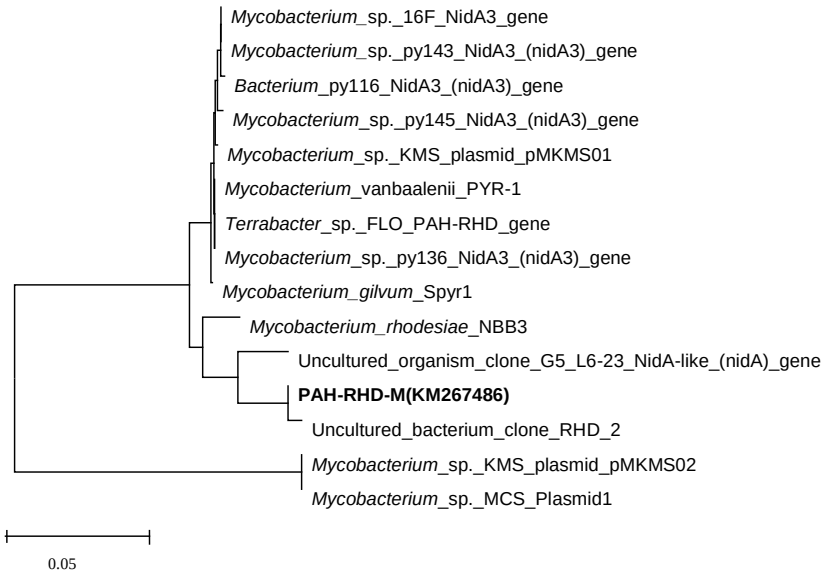

Fig. 2. Phylogenetic tree of PAH-RHDα-M genes from MS (microcosms from Mt. Maoer soil amended with salicylate) and M (microcosms from Mt. Maoer soil without salicylate) treatments along with the closest matches in GenBank, constructed with MEGA 5.0 software using the neighbor-joining method.

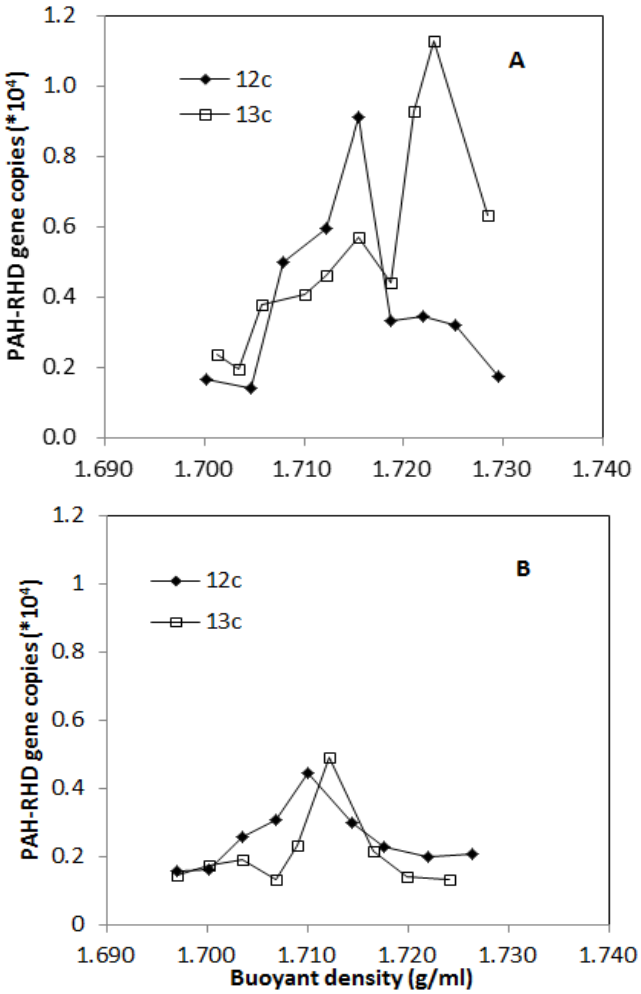

Fig. 3. PAH-RHDα-M gene copies in ultracentrifugation fractions from ^{13}C-BaP and ^{12}C-BaP amended microcosms determined by qPCR. A and B represent the microcosms from Mt. Maoer soil with/without salicylate addition. Figure symbols: □ ^{13}C-BaP (~52% BaP degraded); ■ ^{12}C-BaP (~42% BaP degraded).